Intermittent generalized synchronization and modified system approach: Discrete maps

Alexey A. Koronovskii ⬤,[*] Olga I. Moskalenko ⬤,[†] and Anton O. Selskii[‡]

Institute of Physics, Saratov State University, Saratov 410012, Russia

The present work deals with the intermittent generalized synchronization regime observed near the boundary of generalized synchronization. The intermittent behavior is considered in the context of two observable phenomena, namely, (i) the birth of the asynchronous stages of motion from the complete synchronous state and (ii) the multistability in detection of the synchronous and asynchronous states. The mechanisms governing these phenomena are revealed and described in this paper with the help of the modified system approach for unidirectionally coupled model oscillators with discrete time.

I. INTRODUCTION

The intermittent behavior [1] revealed and studied initially in Lorenz system [2] is well-known to be observed in the nature very widely, from physical [3,4] to living [5–9] and even astronomical [10,11] systems. Researchers who deal with the phenomenon of chaotic synchronization are well-aware that the intermittent behavior precedes arising the synchronous regimes. Indeed, all known types of synchronous dynamics of coupled chaotic systems (to the best of our knowledge) are always accompanied by intermittency, when for the fixed values of the control parameters below the synchronization onset time series of interacting oscillators exhibit alternately both sections of the synchronous behavior (so called "laminar phases") and intervals of the asynchronous dynamics ("turbulent phases," respectively). So, below the onset of the phase synchronization (PS) depending on the parameters of the coupled oscillators type-I, eyelet, and ring intermittencies may be observed [12–14]. Near the boundary of complete (CS) [15] and lag synchronization (LS) [16,17] the phenomenon of on-off intermittency is known to take place. On-off intermittency [18,19] as well as jump intermittency [20] are realized below the generalized synchronization (GS) [21,22] onset. This type of intermittent behavior, where synchronous and asynchronous intervals of motion alternate with each other, observed below the boundary of generalized chaotic synchronization is also called as *"intermittent generalized synchronization"* (IGS). Under certain conditions the mixed intermittency types [23,24] may also take place. In other way, we can say the intermittency should be considered as the core mechanism of transition from the asynchronous to synchronous dynamics.

In this paper, we focus on considering intermittent generalized synchronization as one of the most intriguing types of presynchronous behavior of the GS regime in order to reveal

how intermittent dynamics arises and to explain some of its features.

The structure of our work is the following. In Sec. II, we introduce the basic concepts of the theory of generalized chaotic synchronization (including the intermittent behavior below its boundary), describe the model system used, and formulate two main issues that have remained unresolved so far and require close attention from researchers. Section III is devoted to the core idea of the modified system approach and its adaptation to the system under study. The mechanism being responsible for the laminar and turbulent phase alternations is revealed in Sec. IV. Section V is devoted to the generalization of decision made to multidimensional maps. Section VI deals with the multistability properties observed in the intermittent generalized synchronization regime. Final discussions and remarks are given in Conclusions.

II. PROBLEMS TO BE THOUGHT OVER

A. General theory and model system

As it is well known [21,22], two unidirectionally coupled chaotic systems (say, **x** and **y**) are in the regime of generalized chaotic synchronization if the state of the response system **y** is completely determined by the state of the drive system **x** with the help of functional $\mathcal{F}$

$$\mathbf{y} = \mathcal{F}[\mathbf{x}], \tag{1}$$

with the analytical form of $\mathcal{F}$ being typically unknown.

As a model system in our paper we have mostly used the one-dimensional logistic map

$$x_{n+1} = f(\lambda, x_n), \tag{2}$$

where $f(\lambda, x) = \lambda x(1 - x)$ is the evolution operator and λ is the control parameter. It has long been well-known that two unidirectionally coupled logistic maps (2) exhibit both the generalized synchronization phenomenon and intermittent behavior below the onset of GS [18,25]. Additionally, thanks to its relative simplicity, it allows evident and clear explanations of the phenomena under study. Following Ref. [26], we consider two unidirectionally coupled logistic maps whose

---

[*]Contact author: alexey.koronovskii@gmail.com

[†]Contact author: o.i.moskalenko@gmail.com

[‡]Contact author: selskiiao@gmail.com

dynamics is described by evolution operator

$$x_{n+1} = f(\lambda_d, x_n),$$
$$y_{n+1} = f(\lambda_r, y_n) + \varepsilon(f(\lambda_d, x_n) - f(\lambda_r, y_n)), \tag{3}$$

where x and y are coordinates and λ_d, λ_r are control parameters corresponding to the drive and response systems, respectively. Following Ref. [27], in our work, we have used $\lambda_d = 3.75$, $\lambda_r = 3.79$, since for the given values of control parameters both systems demonstrate developed chaotic dynamics and with the increase of the coupling parameter ε they undergo to the regime of generalized synchronization through intermittent behavior.

As it has been mentioned above, generalized synchronization in unidirectionally coupled oscillators means the presence of the functional $\mathcal{F}$ connecting unambiguously the states of the drive and response systems (of course, after the transient is finished). In our case, the condition of generalized synchronization may be written as

$$y_n = \mathcal{F}(x_n), \tag{4}$$

although the analytical form of functional $\mathcal{F}$ is unknown. The presence of the functional relation between the drive and response systems, and, as a consequence, the existence of the generalized synchronization regime may be revealed by means of several methods, among which the nearest neighbor method [21], the auxiliary system approach [28], the conditional Lyapunov exponent calculation [29] are most often and successfully used.

In the case of unidirectionally coupled systems (just the case considered in this paper), the auxiliary system approach seems to be the simplest, clearest and most effective way to recognize the GS regime. As far as the IGS regime is concerned, the auxiliary system approach is unique technique allowing to detect synchronism between the drive and response oscillators (from the point of view of the GS regime) at any arbitrary chosen moment of (in the considered case, *discrete*) time and, as a consequence, to analyze the intermittent dynamics.

B. Auxiliary system approach and intermittent generalized synchronization

In the framework of the auxiliary system approach, in parallel with the drive and response oscillators the another system (called as *auxiliary* one) must be introduced into consideration, with its evolution operator being equal to the response system, i.e., in the considered case it is

$$z_{n+1} = f(\lambda_a, z_n) + \varepsilon(f(\lambda_d, x_n) - f(\lambda_a, z_n)), \tag{5}$$

where λ_a is the control parameter of the auxiliary system supposed to be equal to λ_r. At the same time, the initial condition, z_0, of the auxiliary system has to differ from the one of the response logistic map, y_0, but to belong to the same basin of attraction as y_0. When the drive and response systems are synchronized from the point of view of the generalized synchronization regime, the states of the response and auxiliary oscillators must coincide with each other due to GS definition (4)
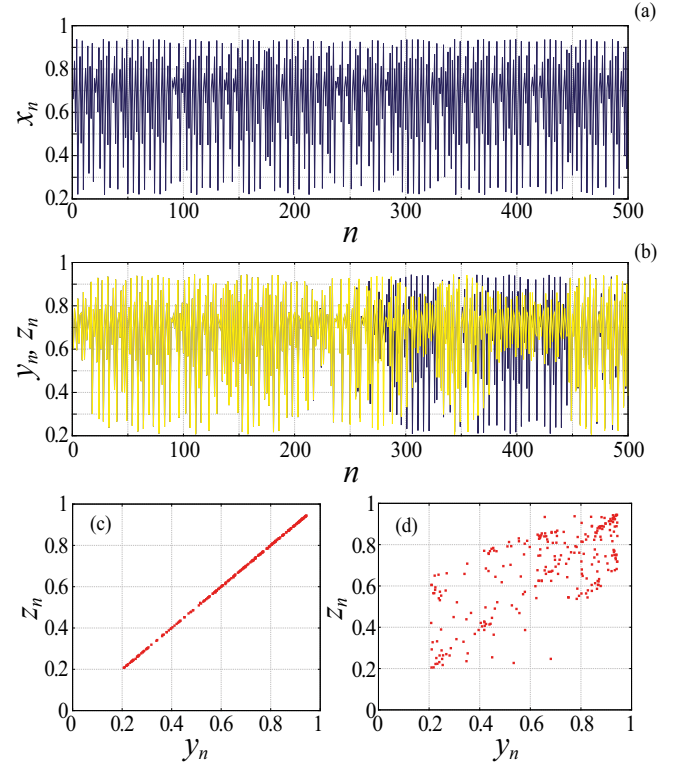
$$y_n = z_n = \mathcal{F}(x_n) \tag{6}$$

FIG. 1. Time series corresponding to the (a) drive x and (b) response y and auxiliary z logistic maps (3), (5) obtained for $\varepsilon = 0.3$. The bottom two plots [(c) and (d)] illustrate the behavior of the response y and auxiliary z systems during the (c) laminar ($n < 275$, $n > 450$) and (d) turbulent ($275 < n < 450$) phases of motion. The transient is omitted.

and identity of the response and auxiliary ones. Alternatively, if there is no synchronization between the drive and response systems, the states of the response and auxiliary oscillators are different ($y_n \neq z_n$ in the case under study). In other words, considering the difference between the coordinates of the response and auxiliary oscillators, $\xi = y - z$, one can easily separate the intervals of synchronous $\xi \simeq 0$ and asynchronous $|\xi| > 0$ behavior bellow the onset of the GS (and, as the next step, one can study the statistical characteristics of intermittency). If the coupling strength value is above the GS threshold, this difference is equal to zero, $\xi = 0$, over all interval of observation that is used in the framework of the auxiliary system approach as the criterion of the GS presence.

The intermittent behavior of unidirectionally coupled logistic maps (3), (5) observed below the onset of GS ($\varepsilon_c \simeq 0.35$) is illustrated in Fig. 1 for the coupling strength $\varepsilon = 0.3$. One can see that the behavior of the drive system differs form the dynamics of the response (as well as the auxiliary) oscillator [compare Figs. 1(a) and 1(b)]. As far as the oscillations in the response and auxiliary maps are concerned [see Figs. 1(b)–1(d)], they may be identical (that is the criterion of laminar phases) or different (that is the indication of turbulent phases) depending on the moment of observation time.

As far as the control parameter value λ_a of the auxiliary system is concerned, its value is typically taken equal to the

response oscillator one, $\lambda_a \equiv \lambda_r$. And if there are no peculiarities in the case of analytical consideration, in the case of numerical simulation one has to take into account that in this situation the threshold ε_c of the GS regime will be slightly underestimated. Indeed, below the true onset of the generalized synchronization where the IGS regime is realized, within the long laminar (synchronous) phase the difference between the response and auxiliary system coordinates ξ may become less than the accuracy of representing a number in computer memory due to its finite digit capacity (so called *counting trap*). After that the states of the response and auxiliary systems in numerical representation with finite digit capacity are absolutely equivalent at any moment of time, therefore, the difference between their states is always equal to zero ($\xi \equiv 0$), and, as a consequence, the GS regime should be detected. At the same time, for the considered coupled oscillators the true small difference ξ between response and auxiliary systems may increase later that results eventually in the interruption of the laminar phase and transition to the turbulent one. To avoid the above mentioned numerical effect, the control parameter value of the auxiliary system may be chosen slightly different from the response system one, $\lambda_a = \lambda_r + \Delta\lambda$, where $|\Delta\lambda/\lambda_r| \ll 1$. Alternative way is the addition of the very small noise signal $|\zeta| \ll y_n$, $\forall n$ to the auxiliary system to make the states of the response and auxiliary oscillators slightly different. Both these approaches (the introduction of a slight parameter mismatch or small noise) represent actually processes taking place in real (not numerical) systems. In our numerical calculations we have used the first of them, namely the introduction of the small parameter mismatch, $\Delta\lambda = 10^{-7}$, to avoid the counting trap caused by the finite digit capacity representation of the system states, while in the analytical consideration we have neglected the small deviation $\Delta\lambda$ and supposed $\lambda_r \equiv \lambda_a$.

C. Two questions

Despite of the fact that both GS phenomenon and IGS regime are now well-studied and described in detail in a lot of scientific papers, there are certain points concerning the IGS phenomenon which are, from one hand, important and, from the other hand, unclear. In the framework of this work, we focus on two interesting and intriguing points that are important for a general understanding of the GS and IGS phenomena.

The first of them is the dynamical mechanisms governing by the completion of the laminar phase and transition to the turbulent one and vice versa. Indeed, why for certain enough long time intervals the response and auxiliary systems move practically identically (synchronous or laminar phase), whereas for other time intervals the states of these systems are significantly different? One would expect that in the generalized phase space of three considered systems (the drive, response, and auxiliary ones) there are some subspaces corresponding to the laminar phases (like the "corridor" between the map function and bisector for the case of type-I intermittency in the quadratic map [1]), however, all our previous attempts (mostly unpublished, except for Ref. [30]) to find these areas in the phase space mentioned above cannot be
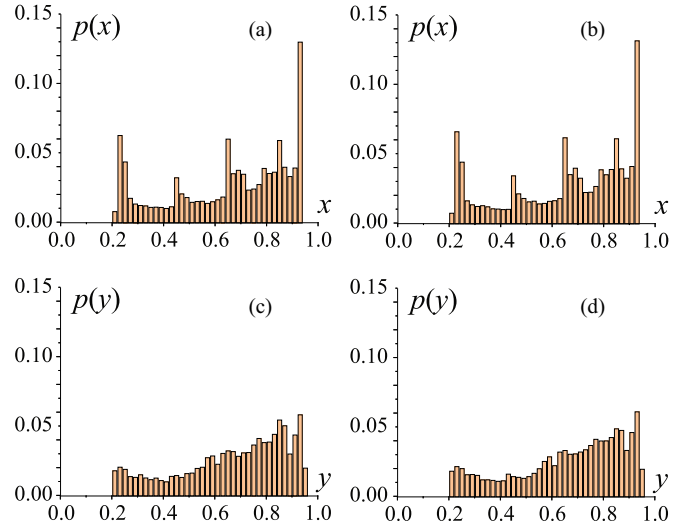

FIG. 2. The probability distributions of the states of the [(a) and (b)] drive and [(c) and (d)] response maps (3) calculated for [(a) and (c)] laminar and [(b) and (d)] turbulent phases, $\varepsilon = 0.3$. The number of points used to calculate each of distributions is $N = 5 \times 10^7$, the width of bin is $\Delta_b = 0.02$

considered as successful. We are also not aware of any similar studies devoted to this topic that have been published so far.

In Fig. 2, the probability distributions for the drive and response logistic maps obtained within the set of laminar [Figs. 2(a) and 2(c)] and turbulent [Figs. 2(b) and 2(d)] phases of motion are given for the coupling strength $\varepsilon = 0.3$. To calculate each of distributions $N = 5 \times 10^7$ points have been used, the width of bin has been chosen as $\Delta_b = 0.02$. All distributions have been normalized to satisfy the normalization condition $\sum_j p_j = 1$. One can easily see that distributions for the laminar and turbulent phases are identical completely which indicates that within synchronous and asynchronous phases of behavior the phase trajectories are located in the same region of the generalized phase space. In other words, the dynamical mechanisms of synchronous and asynchronous motion alternations seem to be unrevealed and, therefore, that is *question 1*, which we are going to answer in our paper.

The second task considered in our paper is related to the newly discovered phenomenon of the multistability near the onset of generalized synchronization in unidirectionally coupled chaotic systems [26]. It has been found that for two unidirectionally coupled chaotic systems being in the IGS regime for one and the same moment of time depending on the initial conditions of the auxiliary system both the synchronous and asynchronous states can be detected. And although some progress has been made in the study and description of multistability in the IGS regime, there is still no explanation of the mechanisms leading to multistability in this case. It is *question 2* which will be answered in this paper.

So, there are two fundamental issues that are addressed in this paper.

(1) Why in the IGS regime two coupled interacting systems being synchronized for a long time start suddenly to exhibit the asynchronous behavior and vice versa (like in Fig. 1)?

(2) Why the intermittent generalized synchronization possesses the multistable properties?

And although at first sight these two mentioned above questions seem to be quite different and independent from each other, the answers to both of them can be given with the help of the modified system approach proposed firstly in Ref. [31]. Moreover, these two questions, as it will be shown below, turn out to be closely related to each other due to this approach. The main idea and adaptation of the modified system technique to the coupled discrete systems under study (3) is given in the next section.

III. THE MODIFIED SYSTEM

According to the methodology proposed and developed in Reef. [31], the GS regime in two unidirectionally coupled oscillators from the point of view of the modified system approach may be considered as a result of superposition of two cooperative mechanisms acting simultaneously. The core idea of the modified system approach [31] is the following. Instead of the response oscillator in Eq. (3) one has to consider *the modified system* which in the case under study is described by

$$u_{n+1} = g(u_n) = (1 - \varepsilon)f(\lambda_r, u_n). \tag{7}$$

So, substituting the modified system (7) for the response one in Eq. (3) one can rewrite evolution operator (3) as

$$y_{n+1} = g(y_n) + \varepsilon f(\lambda_d, x_n). \tag{8}$$

Obviously, obtained Eq. (8) is identical to the second operatior of Eqs. (3) and (5) (with $z \leftrightarrow y$), but now the dynamics of the system under study is clearly divided into two parts, with the coupling parameter increase for each of them realising different mechanisms. With the increase of the coupling strength (parameter ε in our case) (i) the dissipation in the modified system $g(y)$ grows as well as (ii) the amplitude of the external signal enlarges. It is clear that both the processes mentioned above are inextricably linked with each other by means of the coupling parameter and cannot take place in the coupled oscillators independently. At the same time, in the framework of the modified system approach we can consider these both processes separately. In other words, with the help of the modified system method, we can focus our attention on the problem how increasing the coupling parameter ε changes the dynamics of the (modified) response system $g(u)$, leaving the external influence from the response system temporarily out of consideration. It allows us to understand as the causes of the completion of the laminar phase and transition to the turbulent one in the case of the IGS regime as well as the mechanisms leading to multistability in this case.

IV. LAMINAR AND TURBULENT PHASE ALTERNATION

Since all attempts to find the subspaces being responsible for laminar and turbulent phases in the generalized phase space of the drive and response systems seem to be unsuccessful, we are going to explain the phenomenon of intermittent generalized synchronization by considering short time intervals corresponding to the transition from one type of the behavior to another. Therefore we have concentrated on the

end of the laminar phase and the initial section of the transition to asynchronous behavior.

From the analytical point of view, when the synchronous epoch of the drive and response oscillator dynamics is finished and the turbulent motion starts to develop, the small difference between coordinates of the response and auxiliary systems $\xi_n = y_n - z_n$ must increase. One can easily see that the dynamics of this small difference between response and auxiliary oscillators is described by

$$\xi_{n+1} = y_{n+1} - z_{n+1} = g(y_n) - g(z_n). \tag{9}$$

Taking into account that in the end of the laminar phase $|\xi_n| \ll 1$ and

$$\lim_{\xi \to 0} g(z_n) = \lim_{\xi \to 0} g(y_n - \xi_n) = g(y_n) - g'(y_n)\xi_n, \tag{10}$$

from Eqs. (9) and (10), one can obtain

$$\xi_{n+1} = g'(y_n)\xi_n, \tag{11}$$

where $g(y)$ is the evolution operator of the modified system (7). In other words, the dynamics of the small difference between coordinates of the response (3) and auxiliary (5) systems depend at each moment of discrete time on the state of the response oscillator and is determined by evolution operator of the modified system (7). It should also be noted that relation (11) is not applicable when the difference between the states of the response and auxiliary oscillators ceases to be close to zero. In other words, Eq. (11) can only be used within the laminar phases as well as time intervals where the destruction of synchronous motion begins.

In order to increase the difference ξ between the states of the response and the auxiliary logistic maps for the $(n + 1)$th iteration, $|g'(y_n)|$ must be greater than 1. Therefore the range of possible y_n values is divided into three regions: $y < y_1^*$ (region I), $y_1^* < y < y_2^*$ (region II) and $y > y_2^*$ (region III), where

$$y_{1,2}^* = \frac{\lambda_r(1 - \varepsilon) \mp 1}{2\lambda_r(1 - \varepsilon)} \tag{12}$$

are the boundary points separating areas of compression (region II) and stretching (regions I and III) in the phase space of the modified system. For the selected control parameter values ($\varepsilon = 0.3$, $\lambda_r = 3.79$), the boundary points are $y_1 \approx 0.312$ and $y_2 \approx 0.688$. Obviously, the mere fact that the representative point hits the divergence areas I or III does not mean the destruction of the synchronous phase of the behavior. To interrupt the laminar motion the phase trajectory of the response logistic map $\{y_i\}|_{i=n}^{n+L}$ within the short time interval corresponding to the transition from synchronous to asynchronous dynamics (here n is an initial point of the transition, L is the transition length) must be located mostly in regions I and III in comparison with regular (synchronous or asynchronous) behavior.

In Fig. 3(a), the probability distributions $p(y)$ of the states of the response logistic map (3) calculated for the transition from the laminar to turbulent phases of motion are given. Taking into account the multistability phenomenon in the IGS regime, the short time intervals corresponding to this transition, have been selected from the long time series with the help of the calculation of the probability to detect of the asyn-
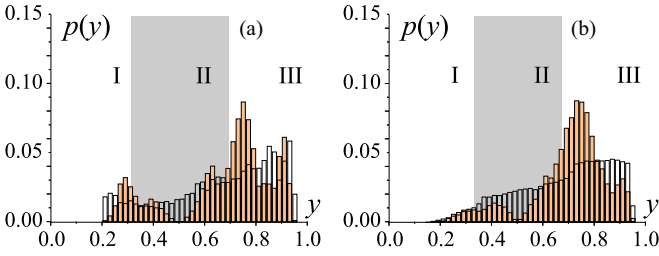
FIG. 3. (a) The probability distributions of the states of the response logistic map (3) calculated for the short time intervals corresponding to the transition from the laminar to turbulent phases of motion (light brown bars) as well as for the laminar phases (transparent bars), $\varepsilon = 0.3$. The gray rectangle corresponds to the area of the phase space of the modified system (7), characterized by the compression of the phase trajectories. (b) The same probability distributions obtained for the noise driven system (13), $\varepsilon = 0.23$. The number of points used to calculate each of distributions is $N = 5 \times 10^7$, the width of bin is $\Delta_b = 0.02$.

chronous regime (24) proposed for the first time in Ref. [26] and described briefly in Sec. VI. The length of transition used for the probability distribution calculation has been taken as $L = 12$. The value of the method parameter L is dictated by the typical time at which the destruction of the synchronous state is observed for the systems under study. Obviously, the choice of an appropriate duration of the transition length is quite important to obtain the correct probability distribution. Choosing a longer time interval means that points belonging to both laminar and turbulent phases will be captured and, therefore, the resulting distribution will be blurred. The longer the used time interval L is, the closer the resulting distribution is to the distribution plotted over the whole time series, and, consequently, the less pronounced the desired effect is. On the contrary, a reduction of the transition length L results in poor statistics and associated distortions of the calculated distribution. For comparison, in the same figure the probability density distribution of the response system [see Fig. 2(c)] obtained for the laminar phases only is also shown by transparent rectangles. In contrast to the previous one, this distribution is plotted over intervals of time series with different lengths corresponding to the durations of the analysed laminar phases.

As one can see from Fig. 3(a) for the transition epoch the probability distribution $p(y)$ radically changes its shape in comparison with the laminar and turbulent phases. The probability for the phase trajectory located in the compression region II decreases sufficiently and in the vicinity of the point $y_e = 0.5$, where $g'(y_e) \to 0$, this probability is generally close to zero. So, we come to the conclusion that in the time series of the response system $\{y_n\}$ rather short segments sometimes occur, where the majority of points are located in the phase space regions (in the considered case, in regions I and III) characterized by a divergence of neighbor trajectories. Within this short interval of discrete time the phase trajectories of the response and auxiliary systems diverge by a distance being sufficient for the time series of these systems to become noticeably different, which, in turn, triggers the turbulent phase.

It is also interesting to note some asymmetry in the behavior of the distributions $p(y)$ in regions I and III. One can see from Fig. 3 that for the transitions from synchronous to asynchronous dynamics, a significant number of new points appear in region III, while the changes in region I are not practically noticeable. This asymmetry is explained by the fact that a larger fraction of points of the chaotic attractor of the system under study is located in region III in comparison with region I. However, the key factor of the synchronous behavior destruction is not an increase in the number of distribution points in regions I and III, but a significant decrease in the number of points in region II, with such points that corresponding to the areas of maximal convergence of close phase trajectories (see areas in Figs. 3(a) and 3(b) near the point $y_e = 0.5$, where $g'(y_e) = 0$).

Given that it has been previously shown [32–34] that the phenomenon of *noise-induced synchronization* [35–37] is caused by the same mechanisms as generalized synchronization, one can expect that the above discussed features of the systems behavior revealed below the onset of the synchronous regime should be also observed for oscillators under the random signal. To confirm this assumption, we replace the signal of the drive oscillator in the example under study by a random variable ζ_n distributed uniformly in the range [0; 1]

$$y_{n+1} = f(\lambda_r, y_n) + \varepsilon(f(\lambda_d, \zeta_n) - f(\lambda_r, y_n)),$$
$$z_{n+1} = f(\lambda_a, z_n) + \varepsilon(f(\lambda_d, \zeta_n) - f(\lambda_a, z_n)). \quad (13)$$

As one might expect, in system (13), at certain values of parameter $\varepsilon \geqslant \varepsilon_c = 0.26$, there is also a completely synchronous dynamics between the response and auxiliary oscillators ($y_n = z_n$) and, therefore, from a formal point of view, system (13) exhibits a *noise-induced synchronization* regime. Below a threshold value of ε_c, there is an intermittent behavior being identical to the intermittent generalized synchronization observed in (3), (5).

Although for Eqs. (13) time series of the response and auxiliary systems are randomized, in these time series, as well as for deterministic oscillators (3) and (5), there are also short intervals in which points are mostly located in the phase space regions I and III, where the divergence of the phase trajectories takes place. It is these segments of time series $\{y_i\}|_{i=n}^{n+L}$ that complete the laminar phases of the behavior and start the phases of asynchronous (turbulent) dynamics. The probability distributions obtained for these short transition intervals (light brown bars) in comparison with the laminar phases (transparent bars) are given in Fig. 3(b). One can see that these distributions $p(y)$ obtained for the deterministic [Fig. 3(a)] and random [Fig. 3(b)] drive signals are qualitatively equivalent.

Taking into account the obtained results, it can be assumed that the occurrence of sequences $\{y_i\}|_{i=n}^{n+L}$ obeys probabilistic regularities. In other words, in the time series of the response oscillator relatively short sequences $\{y_i\}|_{i=n}^{n+L}$ appear among the entire set of points y_n which triggers turbulent phases, with the probability of such sequences occurrence decreasing with the growth of the coupling parameter ε. In order to test the probabilistic nature of the occurrence of these sequences $\{y_i\}|_{i=n}^{n+L}$, we consider the behavior of the difference ξ_n between two neighbor trajectories governed by linearized Eq. (11), but instead of the coordinates y_n of the response system we use a random sequence ζ_n with the uniform probability distribution within the range [0; 1]. In other words, we emulate
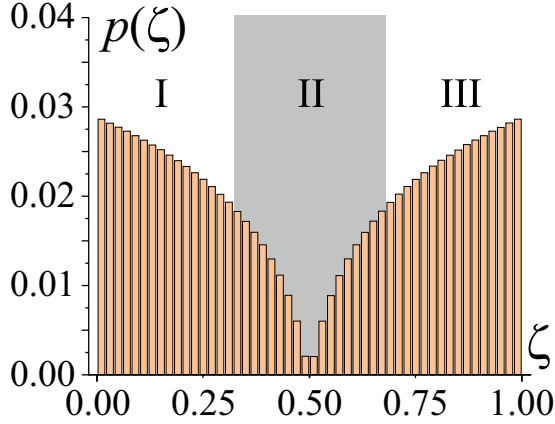
FIG. 4. The probability distribution $p(\zeta)$ of the random points ζ_n corresponding to transitions from the laminar to turbulent phases of motion. The gray rectangle corresponds to the area of the phase space of the modified system (7), characterized by the compression of the phase trajectories. The number of points used to calculate distribution is $N = 5 \times 10^7$, the width of bin is $\Delta_b = 0.02$. The control parameter of modified system are $\lambda = 3.79$, $\varepsilon = 0.3$.
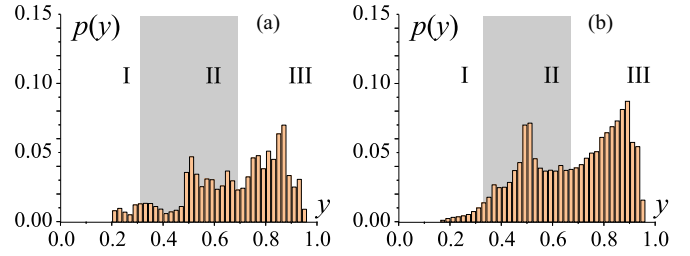

FIG. 5. (a) The probability distribution of the states of the response logistic map (3) calculated for the short time intervals corresponding to the transition from the turbulent to laminar phases of motion (light brown bars), $\varepsilon = 0.3$. The gray rectangle corresponds to the area of the phase space of the modified system (7), characterized by the compression of the phase trajectories. (b) The same probability distribution obtained for the noise driven system (13), $\varepsilon = 0.23$. The number of points used to calculate each of distributions is $N = 5 \times 10^7$, the width of bin is $\Delta_b = 0.02$.

the chaotic (but deterministic) time series y_n by completely random surrogate signal ζ_n. Further, considering sequentially all segments $\{\zeta_i\}|_{i=n}^{n+L}$ with length L of the random sequence ζ_n, we will choose only those for which the distance ξ_n increases by more than K_1 times (i.e., $\xi_{n+L}/\xi_n > K$) and consider them as short time intervals corresponding to transitions from laminar phases to turbulent ones just like in cases of coupled logistic maps (3) and logistic maps driven by noise (13). In our study, we have used $K = 10$ that corresponds to a significant divergence of the initially adjacent trajectories.

In Fig. 4, the probability distributions $p(\zeta)$ of the random surrogate points assigned to intervals emulating the transitions from laminar to turbulent phases are shown. One can see, that despite of the completely random nature of the surrogate signal ζ_n, the qualitative form of the distribution $p(\zeta)$ of points corresponding to transitions from laminar to turbulent phases happens to be exactly the same as for the cases of coupled logistic maps (3) and logistic maps driven by noise (13). Figure 4 clearly shows a pronounced minimum of the probability density $p(\zeta)$, located in the region around $\zeta_e = 0.5$ where the maximum strong compression of phase trajectories takes place. The apparent identity of the probability densities $p(y)$ and $p(\zeta)$ given in Figs. 3 and 4 convincingly confirms the probabilistic nature of the phenomenon observed.

So, just below the synchronization onset in the phase trajectory of the response system with a certain (small) probability there are short sections mostly lying in the regions of the phase space, which for the modified system are areas of divergence of the close phase trajectories. There are these sections of the phase trajectories that are responsible for the divergence of the initially close trajectories of the response and auxiliary systems at a considerable distance from each other, after which the phase trajectories of these systems become different, which results in the detection of the turbulent phase.

It should also be noted that the backward transitions from turbulent to laminar phases are also associated with the ran-

domly occurring short segments of the phase trajectory of the response system, which, in turn, are mostly located in the area of the modified system phase space where the compression takes place, including the region with the maximal one (for the system under consideration it is the region in the vicinity of $y_e = 0.5$, where $g'(y_e) \simeq 0$). The probability distributions obtained for these intervals for the deterministic (a) and random (b) driven signals are shown in Fig. 5. In both cases, contrary to the transition from laminar to turbulent phases, a very pronounced peak of the probability distribution $p(y)$ is clearly visible in region II, at $y_e = 0.5$.

Now, having a clear understanding of the mechanisms that results in the alternation of laminar and turbulent phases near the synchronization onset, it remains for us to answer one important question, namely, why does the transition to fully synchronous dynamics occur with an increase of the coupling parameter ε?

It is obvious that, firstly, with an increase of the control parameter ε, there is a gradual expansion of region II (and, accordingly, a compression of regions I and III). Accordingly, some part of the points that, at a lower value of the coupling parameter ε, fell into the regions of scattering of initially close phase trajectories (regions I and III), with an increase of the coupling strength, start to be located in region II, characterized by the compression of the phase space. Secondly, those points of the trajectory of the driven system, which still fall into the regions of the phase trajectories divergence, for the same value of y are characterized by a smaller degree of divergence of close phase trajectories, $|g'(y)|$. The combination of these two factors decreases the probability of the appearance of segments of the phase trajectory, the representing points of which are located mainly in the divergence regions, that, in turn, for a certain (critical) coupling parameter value, ε_c, results in the transition to a completely synchronous generalized synchronization regime.

V. THE CASE OF N-DIMENSIONAL MAPS

The use of the modified system approach to explain the mechanism of intermittent generalized synchronization described in the previous Sec. IV can be generalized

to the case of N-dimensional unidirectionally coupled maps with the dissipative coupling. Indeed, let N-dimensional vectors $\mathbf{x} = (x_1, x_2, \ldots, x_N)^T$, $\mathbf{y} = (y_1, y_2, \ldots, y_N)^T$, $\mathbf{z} = (z_1, z_2, \ldots, z_N)^T$ be the states of the drive, response and auxiliary systems, respectively. The dynamics of the drive and response systems are determined by the following evolution operators:

$$\mathbf{x}_{n+1} = \mathbf{F}^d(\mathbf{x}_n, \mathbf{p}^d) \qquad (14)$$

and

$$\mathbf{y}_{n+1} = \mathbf{F}(\mathbf{y}_n, \mathbf{p}^r) + \varepsilon\mathbf{A}(\mathbf{F}^d(\mathbf{x}_n, \mathbf{p}^d) - \mathbf{F}(\mathbf{y}_n, \mathbf{p}^r)), \qquad (15)$$

where $\mathbf{F}^d = (F_1^d, \ldots, F_N^d)^T$ and $\mathbf{F} = (F_1, \ldots, F_N)^T$ are the N-dimensional vector-functions, $\mathbf{p}^d$ and $\mathbf{p}^r$ — the control parameter vectors of the drive and response maps, respectively. $\mathbf{A} = \{a_{ij}\}$ ($a_{ij} = 0$ or 1) is the dissipative coupling matrix. The auxiliary system is also determined by Eq. (15) with substitutions of the quantities $\mathbf{z}$ for $\mathbf{y}$ and $\mathbf{p}^a$ for $\mathbf{p}^r$, ($\mathbf{p}^a = \mathbf{p}^r + \Delta\mathbf{p}$, $||\Delta\mathbf{p}|| \to 0$). The modified system for the considered N-dimensional map is

$$\mathbf{u}_{n+1} = \mathbf{G}(\mathbf{u}_n) = (\mathbf{E} - \varepsilon\mathbf{A})\mathbf{F}(\mathbf{u}_n, \mathbf{p}^r), \qquad (16)$$

where $\mathbf{G} = (G_1, \ldots, G_N)^T$ is n-dimensional vector-function, $\mathbf{E}$ is an n-dimensional unit matrix, $e_{ij} = 1$ if $i = j$ and 0 otherwise. As well as in the case of one-dimensional maps (see previous Sec. IV), the small differences between coordinates of the response and auxiliary systems decrease at those points $\mathbf{y}_n$ of the N-dimensional phase space of the response system for which

$$|\mu_i| < 1, \quad \forall i = 1, \ldots, N, \qquad (17)$$

where μ_i are the eigenvalues of matrix

$$J\mathbf{G} = \begin{pmatrix} \frac{\partial G_1}{\partial u_1} & \frac{\partial G_1}{\partial u_2} & \cdots & \frac{\partial G_1}{\partial u_N} \\ \frac{\partial G_2}{\partial u_1} & \frac{\partial G_2}{\partial u_2} & \cdots & \frac{\partial G_2}{\partial u_N} \\ \vdots & \vdots & \ddots & \vdots \\ \frac{\partial G_N}{\partial u_1} & \frac{\partial G_N}{\partial u_2} & \cdots & \frac{\partial G_N}{\partial u_N} \end{pmatrix}\Bigg|_{\mathbf{u}=\mathbf{y}_n} \qquad (18)$$

and increase otherwise [if at least one of the values $|\mu_i|$ ($i = 1, \ldots, N$) is greater than 1]. Again, as well as in the case of one-dimensional maps the laminar motion is interrupted when the phase trajectory of the response map $\{\mathbf{y}_i\}|_{i=n}^{i=n+L}$ within the short time interval corresponding to the transition from synchronous to asynchronous dynamics (here n is an initial point of the transition, L is the transition length) is located mostly in subspaces of the phase space characterized by the divergence of phase trajectories (i.e., where $\exists i, |\mu_i| > 1$) in comparison with regular (synchronous or asynchronous) behavior.

We illustrate the described generalized approach to multidimensional discrete systems with the example of a two-dimensional Hénon map [38]. In this case, the vector-function of the drive system is

$$\mathbf{F}^d(\mathbf{x}, \mathbf{p}^d) = \begin{pmatrix} 1 - p_1^d x_1^2 + x_2 \\ p_2^d x_1 \end{pmatrix}, \qquad (19)$$

the vector-function for the response system is given by

$$\mathbf{F}(\mathbf{y}, \mathbf{p}^r) = \begin{pmatrix} 1 - p_1^r y_1^2 + y_2 \\ p_2^r y_1 \end{pmatrix} \qquad (20)$$

and the coupling matrix is chosen as

$$\mathbf{A} = \begin{pmatrix} 1 & 0 \\ 0 & 0 \end{pmatrix}. \qquad (21)$$

For the selected values of the control parameters $p_1^d = 1.4$, $p_1^r = 1.35$, $p_2^d = p_2^r = 0.3$ the autonomous ($\varepsilon = 0$) Hénon maps demonstrate the chaotic behavior. With the growth of the coupling strength ε the coupled systems undergo to the generalized synchronization regime at $\varepsilon_c = 0.34$, whereas just below the boundary of GS the intermittent behavior (intermittent generalized synchronization) is observed.

The eigenvalues of the matrix $J\mathbf{G}$ in the considered case are

$$\mu_{1,2} = (1 - \varepsilon)\left(\pm\sqrt{(p_1^r y_1)^2 - \frac{p_2^r}{1 - \varepsilon}} - p_1^r y_1\right) \qquad (22)$$

and, as it can be seen, $\mu_{1,2}$ depend only on the first coordinate of the response system, y_1. Accordingly, we can now consider the projection of phase space of the response system on the y_1 axis and divide it into regions of compression and stretching of phase trajectories, respectively. According to criterion (17) the projection of the response map phase space y_1 (and, the whole phase space, accordingly) is divided into three subspaces: $y_1 < -y^*$ (region I), $-y^* < y_1 < y^*$ (region II) and $y^* < y_1$ (region III), where

$$y^* = \frac{1 + p_2^r(1 - \varepsilon)}{2p_1^r(1 - \varepsilon)}. \qquad (23)$$

For the selected control parameters, the boundary point value is $y^* \approx 0.64$. Regions I and III are responsible for the divergence of the close phase trajectories, while region II, on the contrary, provides a reduction in the distance between such trajectories.

In Fig. 6, the probability distribution $p(y_1)$ of the response Hénon map (20) calculated for the transition intervals from the laminar to turbulent phases of motion is shown by light brown bars. The length of transition used for the calculation has been chosen the same as in the case of logistic maps considered above ($L = 12$). Again, for comparison, in the same figure the probability density distribution of the response system obtained for the laminar phases only is shown by transparent rectangles. Obviously, just as in the case of one-dimensional maps described above (Sec. IV), in the considered case for the time intervals of transition from laminar phases to turbulent ones it is clearly seen a sharply pronounced change in the character of the distribution $p(y_1)$. From Fig. 6, one can see a radical reduction in the number of points in region II being responsible for the convergence of close phase trajectories.

Thus, after considering the intermittent behavior in unidirectionally coupled Hénon maps below the threshold of the GS regime, we can conclude that in multidimensional systems (in the case under consideration, two-dimensional) the same mechanism that has been revealed on the example of one-dimensional logistic maps is responsible for the emergence
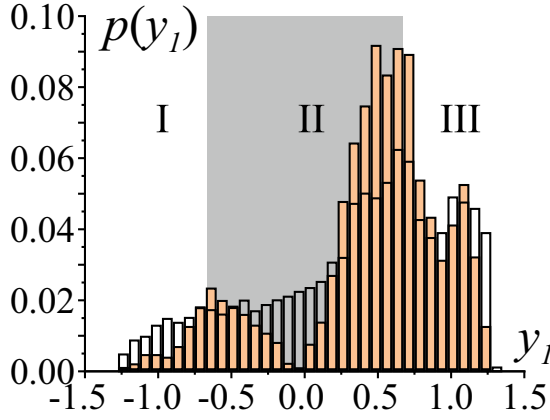
FIG. 6. The probability distribution of the y_1 coordinates of the response Hénon map (20) with coupling term given by matrix (21) calculated for the short time intervals corresponding to the transition from the laminar to turbulent phases of motion (light brown bars) in comparison with the analogous distribution obtained for laminar phases (transparent bars), $\varepsilon = 0.3$. The gray rectangle corresponds to the area of the phase space, characterized by the compression of the phase trajectories (region II). The number of points used to calculate each of distributions is $N = 5 \times 10^7$, the width of bin is $\Delta_b = 0.02$.

of alternating epochs of the synchronous and asynchronous behavior. This, in turn, allows us to speak on the universality of the revealed mechanism and the possibility of using it to describe, both qualitatively and quantitatively, the phenomenon of intermittent generalized synchronization in discrete-time dynamical systems of arbitrary dimension. In addition, due to the connection between the flows and the maps via the Poincaré secant method [39], it is hoped that the developed technique may serve as a bridge to the understanding of the mechanisms that lead to the emergence of the IGS regime in flow systems.

VI. MULTISTABILITY IN THE IGS REGIME

Let us now move to the consideration of question 2 and try to answer where the multistability in the intermittent generalized synchronization regime comes from. As well as it is known [26], for the regime of intermittent generalized synchronization in certain periods of time the current stage may be detected as both synchronous and asynchronous motion depending on the choice of initial condition of the selected auxiliary system. To describe quantitatively the revealed intermittency phenomenon in Ref. [26] the probability of the detection of the asynchronous regime in the nth moment of discrete time P_n^a has been proposed. This measure of multistability may be calculated for the set of $N \to \infty$ identical (with the precision to $\Delta\lambda$) response systems y_n^j ($j = 1, \ldots, N$) as

$$P_n^a = 1 - \sum_{j=1}^{N} \frac{n(y_n^j)}{N(N-1)}, \qquad (24)$$

where $n(y_n^j)$ is a number of the response oscillators being in the identical state with jth response oscillator y_n^j at the moment of discrete time n. At the beginning, the initial conditions of all oscillators under consideration may be chosen arbitrarily

from the basin of attraction of the chaotic attractor of the autonomous system, providing that all initial points are different. After a long transient process (we have used $T_{tr} = 10^5$), when the regime of intermittent generalized chaotic synchronization is considered to be fully established, the measure of multistability P_n^a may be calculated. Two response oscillators, y_n^j and y_n^k, are assumed to be in identical states at the moment of discrete time n with the accuracy of elementary volume $\delta \ll 1$ in the phase space $x \in (0; 1)$ if

$$\left| y_n^j - y_n^k \right| < \delta. \qquad (25)$$

Due to its probabilistic approach Eq. (24) is closely connected to the concept of "tipping probabilities" used to describe the rate-tipping phenomena [40].

If P_n^a is equal to zero, it means that all considered response oscillators are in one and the same state and the synchronous phase of dynamics is realized in the unidirectionally coupled logistic maps. The closer the value of $P_n^a > 0$ is to unity, the greater is the probability of detecting the turbulent phase with the help of the auxiliary system method. Having calculated the dependence of P_n^a on the discrete time n one can easily separate the epochs of the synchronous and asynchronous behavior as well as the segments of the transitions between these phases. Indeed, at discrete time n_{end}^l, when the value of P_n^a, which was below some predetermined threshold value P_c, begins to exceed this value, the moment of completion of the laminar phase is fixed. After this moment of discrete time the interval of duration L begins, during which the laminar phase is destroyed and the transition to the turbulent phase is realized. In this case, the beginning of the developed turbulent phase is $n_{\text{start}}^t = n_{\text{end}}^l + L$. Conversely, the moment of discrete time n_{start}^l, when the value of P_n^a, which exceeded previously the critical level P_c, happens to be below it (and then stays below this critical value during the following L iterations), is considered as the beginning of the laminar phase, whereas the moment of the turbulent phase destruction is fixed as $n_{\text{end}}^t = n_{\text{start}}^l - L$. The interval of L discrete units between n_{end}^t and n_{start}^l corresponds to the transition from turbulent (asynchronous) to laminar (synchronous) behavior. It is the approach that has been used in Sec. IV to calculate the probability distributions for the different types of dynamics of unidirectionally coupled logistic maps (3), logistic maps driven by the random signal (13) and coupled Hénon maps (14) and (15). The threshold value in our consideration has been fixed as $P_c = 10^{-3}$ for coupled logistic maps and Hénon maps. Due to the noise influence for logistic maps driven by random signal the threshold value should be enlarged, therefore, in this case, it has been chosen as $P_c = 5 \times 10^{-2}$.

To reveal the underlying mechanism of the multistability manifestation in the intermittent generalized synchronization regime, we turn to the consideration of the modified system (7) again. For the control parameter values $\lambda_r = 3.79$ and $\varepsilon = 0.3$ used in our work and corresponding to the IGS regime, the attractor of the autonomous modified system is the stable fixed point

$$u_0 = \frac{\lambda(1-\varepsilon) - 1}{\lambda(1-\varepsilon)}. \qquad (26)$$

If one consider the term $\varepsilon f(\lambda_d, x_n)$ in Eq. (8) as the additional control parameter $h \in [0; \varepsilon)]$ of the modified system

$$u_{n+1} = g(u_n) + h = (1 - \varepsilon)f(\lambda_r, u_n) + h, \qquad (27)$$

the attractors of this modified system are the stable fixed point

$$u_0 = \frac{\sqrt{4\lambda h(1 - \varepsilon)\varepsilon + (\lambda(1 - \varepsilon) - 1)^2} + \lambda(1 - \varepsilon) - 1}{2\lambda(1 - \varepsilon)} \qquad (28)$$

for

$$h < h_c = \frac{(\lambda(1 - \varepsilon) + 1)(3 - \lambda(1 - \varepsilon))}{4\lambda(1 - \varepsilon)\varepsilon} \approx 0.3982 \qquad (29)$$

and stable 2-cycle, otherwise, if $h > h_c$. It is clear that since the parameter h depends on the state of the drive system x_n and varies greatly from the iteration to iteration, the attractor of the modified system is also rebuilt at each moment of discrete time n, so the system is always in the state of an unfinished transient. Nevertheless, the modified system is highly dissipative and, in turn, the ensemble of N response systems y_n^j ($j = 1, \ldots, N$) will tend to collapse to one and the same state y_n which should correspond to the generalized synchronization regime. In fact, this is exactly what happens during the laminar phase, when all response systems are assembled into one compact cluster.

However, there are several factors preventing the establishment of a fully synchronous regime. *The first* of them is the passage of phase trajectories of the response systems through the short intervals, characterized by a significant divergence of the neighbor trajectories and being responsible for the transition from the synchronous phase to the asynchronous one, which has been described above in the Secs. IV and V. After passing through such intervals, the states of the response systems y_n^j are, as a rule, still within the same cluster, however, its size becomes significantly larger. As a result, when one determines the synchronism with some predetermined accuracy δ, the synchronization is still detected between some response systems, but between some ones it is no longer exist. Accordingly, the probability to detect a turbulent phase P_n^a increases in parallel with the multistability effect begins to be observed.

The second factor supporting the existence of turbulent phases and, accordingly, intermittent behavior near the onset of GS, is the permanent rearrangement of the attractor of the modified and, accordingly, the response systems (due to the dynamics of the drive oscillator), which prevents the states of the ensemble of response systems from rapidly collapsing back into a highly localized area corresponding to the synchronous regime. And *the third* one is the limit cycle of period two that occurs from time to time in the modified system phase space due to the evolution of the control parameter h (i.e., due to the dynamics of the drive oscillator), the appearance of which can break up the existing cluster of the response system states into several ones. It is important to note that the observed behavior is very closely related to the concepts of multiscale systems, critical manifolds and rate tipping points and has some features in common with tipping phenomena in
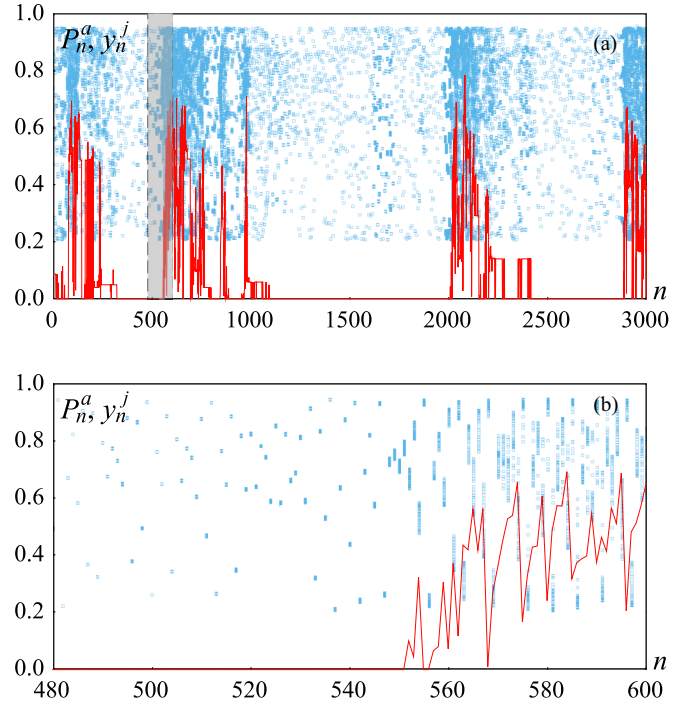

FIG. 7. (a) The dependence of the probability to detect the turbulent (the asynchronous) motion P_n^a on the discrete time n (the solid red line) and the coordinates y_n^j of $N = 250$ response systems (blue points), $\varepsilon = 0.3$. (b) The short fragment of Fig. 7(a).

dynamical systems, whith the state of the drive system plaing the role of the drift parameter [40].

All three factors described above one can easily see from Figs. 7 and 8. In Fig. 7(a), the dependence of the probability to detect the turbulent (the asynchronous) motion P_n^a on the discrete time n is shown. The given fragment is chosen to be sufficiently long, and, therefore, it covers several phases
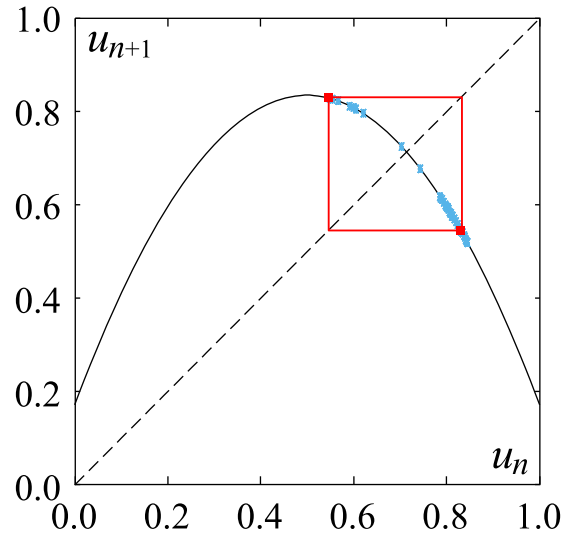

FIG. 8. The typical distribution of the states of the response oscillator cluster (blue points) on the Lamerey diagram of the modified system (27) for the case when the stable 2-cycle (red points and rectangle) is the attractor in the modified oscillator, $\varepsilon = 0.3$, $h = 0.172$.

of both the laminar and turbulent motion. The shorter time interval corresponding to the transition from the laminar to turbulent phase is shown in Fig. 7(b) [this fragment is marked by the gray rectangle in Fig. 7(a)]. In both Figs. 7(a) and 7(b) in parallel with P_n^a, the coordinates y_n^j of N response systems are shown by blue points. For illustration and clarity, the number of the response systems was chosen to be relatively small, $N = 250$. One can see that within the laminar phase all response systems form the localized cluster and, as a consequence, the probability (24) to detect the turbulent phase with the predetermined accuracy $\delta = 5 \times 10^{-2}$ is equal to zero. At the same time, out of the laminar phases the coordinates of the response oscillators are localized within one or several clusters whose size exceeds the accuracy δ that, in turn, results in the growth of P_n^a value and the manifestation of the multistability, respectively.

In Fig. 8, the typical distribution of the response oscillator states y_n^j on the Lamerey diagram of the modified system is shown for the case when (due to the control parameter values) the attractor of the modified system is the stable cycle with period of 2. The elements of the stable periodic cycle are shown as two red points connected by the red square representing periodic oscillations in Lamerey diagram. One can see that all points y_n^j representing the states of the response systems are divided into two extended clusters each of them is attracting to one of two elements of periodic 2-cycle. Obviously, such stretching of the set of potential locations of the response systems in the phase space results in a significant increase in the value of P_n^a and, accordingly, a noticeable manifestation of the multistability properties in the regime of the intermittent generalized synchronization.

VII. CONCLUSIONS

In conclusion, in the present paper we have described the mechanisms of the intermittent generalized synchronization regime observed near the boundary of generalized synchronization in unidirectionally coupled discrete maps. Having considered the features of the behavior of coupled logistic maps, we have explained the causes of the turbulent phases as well as multistability emergence. Taking into account the close relationship between systems with continuous and discrete time, one can reasonably expect that the mechanisms identified and described in this paper for the coupled maps may to some extent determine the features of intermittent behavior near the boundary of generalized chaotic synchronization in the coupled chaotic oscillators with continuous time. At the same time, due to the characteristic features of flow systems and their significant differences from maps, it is obvious that the direct "mechanical" transfer of the regularities found for maps to flow systems does not seem to be reasonable, and, accordingly, the analysis of the behavior of coupled flow oscillators near the boundary of the generalized chaotic synchronization regime requires the additional efforts and deserves the separate consideration.

ACKNOWLEDGMENTS

[1] P. Berge, Y. Pomeau, and C. Vidal, *Order within Chaos* (John Wiley and Sons, New York, 1984).

[2] P. Manneville and Y. Pomeau, Phys. Lett. A **75**, 1 (1979).

[3] I. M. Kyprianidis, M. L. Petrani, J. A. Kalomiros, and A. N. Anagnostopoulos, Phys. Rev. E **52**, 2268 (1995).

[4] A. N. Pisarchik, A. V. Kir'yanov, Y. O. Barmenkov, and R. Jaimes-Reategui, J. Opt. Soc. Am. B **22**, 2107 (2005).

[5] J. L. P. Velazquez, H. Khosravani, A. Lozano, B. L. Bardakjian, P. L. Carlen, and R. Wennberg, Eur. J. Neurosci. **11**, 2571 (1999).

[6] J. L. Cabrera and J. G. Milton, Phys. Rev. Lett. **89**, 158702 (2002).

[7] C. Park, R. M. Worth, and L. L. Rubchinsky, Phys. Rev. E **83**, 042901 (2011).

[8] P. Gong, A. R. Nikolaev, and C. van Leeuwen, Phys. Rev. E **76**, 011904 (2007).

[9] S. Ahn, C. Park, and L. L. Rubchinsky, Phys. Rev. E **84**, 016201 (2011).

[10] R. A. Miranda, E. L. Rempel, and A. C.-L. Chian, Mon. Not. R. Astron. Soc. **448**, 804 (2015).

[11] A. Wawrzaszek and M. Echim, Front. Astron. Space Sci. **7**, 617113 (2021).

[12] A. S. Pikovsky, G. V. Osipov, M. G. Rosenblum, M. Zaks, and J. Kurths, Phys. Rev. Lett. **79**, 47 (1997).

[13] S. Boccaletti, E. Allaria, R. Meucci, and F. T. Arecchi, Phys. Rev. Lett. **89**, 194101 (2002).

[14] A. E. Hramov, A. A. Koronovskii, M. K. Kurovskaya, and S. Boccaletti, Phys. Rev. Lett. **97**, 114101 (2006).

[15] C.-M. Kim, Phys. Rev. E **56**, 3697 (1997).

[16] M. G. Rosenblum, A. S. Pikovsky, and J. Kurths, Phys. Rev. Lett. **78**, 4193 (1997).

[17] S. Boccaletti and D. L. Valladares, Phys. Rev. E **62**, 7497 (2000).

[18] K. Pyragas, Nonlin. Analys.: Model. and Control **3**, 101 (1998).

[19] A. E. Hramov and A. A. Koronovskii, Europhys. Lett. **70**, 169 (2005).

[20] A. A. Koronovskii, O. I. Moskalenko, A. A. Pivovarov, V. A. Khanadeev, A. E. Hramov, and A. N. Pisarchik, Phys. Rev. E **102**, 012205 (2020).

[21] N. F. Rulkov, M. M. Sushchik, L. S. Tsimring, and H. D. I. Abarbanel, Phys. Rev. E **51**, 980 (1995).

[22] N. F. Rulkov, Chaos **6**, 262 (1996).

[23] A. E. Hramov, A. A. Koronovskii, O. I. Moskalenko, M. O. Zhuravlev, V. I. Ponomarenko, and M. D. Prokhorov, CHAOS **23**, 033129 (2013).

[24] A. A. Koronovskii, A. E. Hramov, V. V. Grubov, O. I. Moskalenko, E. Sitnikova, and A. N. Pavlov, Phys. Rev. E **93**, 032220 (2016).

[25] K. Pyragas, Phys. Rev. E **54**, R4508(R) (1996).

[26] O. I. Moskalenko, A. A. Koronovskii, A. O. Selskii, and E. V. Evstifeev, Chaos **31**, 083106 (2021).

[27] A. A. Koronovskii, O. I. Moskalenko, S. A. Shurygina, and A. E. Hramov, Chaos Solitons Fractals **46**, 12 (2013).

[28] H. D. I. Abarbanel, N. F. Rulkov, and M. M. Sushchik, Phys. Rev. E **53**, 4528 (1996).

[29] K. Pyragas, Phys. Rev. E **56**, 5183 (1997).

[30] A. A. Koronovskii, O. I. Moskalenko, A. A. Pivovarov, and A. E. Hramov, Tech. Phys. Lett. **43**, 328 (2017).

[31] A. E. Hramov and A. A. Koronovskii, Phys. Rev. E **71**, 067201 (2005).

[32] A. E. Hramov, A. A. Koronovskii, and O. I. Moskalenko, Phys. Lett. A **354**, 423 (2006).

[33] O. I. Moskalenko, A. A. Koronovskii, and S. A. Shurygina, Tech. Phys. Lett. **56**, 1369 (2011).

[34] E. D. Illarionova and O. I. Moskalenko, Izvestiya VUZ. Applied Nonlinear Dynamics **31**, 566 (2023).

[35] A. Maritan and J. R. Banavar, Phys. Rev. Lett. **72**, 1451 (1994).

[36] Y. Y. Chen, Phys. Rev. Lett. **77**, 4318 (1996).

[37] R. Toral, C. R. Mirasso, E. Hernández-Garsia, and O. Piro, Chaos **11**, 665 (2001).

[38] M. Hénon, Commun. Math. Phys. **50**, 69 (1976).

[39] M. Hénon, Physica D **5**, 412 (1982).

[40] B. Kaszás, U. Feudel, and T. Tél, Sci. Rep. **9**, 8654 (2019).